Plastic deformation of multicrystalline thin films: grain size distribution vs. grain orientation

http://dx.doi.org/10.1016/j.commatsci.2011.03.001

Plastic deformation of Multicrystalline Thin Films: Grain Size Distribution vs. Grain Orientation

Saurabh Puri[1], Anish Roy[2]

[1]Department of Mechanical Engineering,
California Institute of Technology, Pasadena, CA 91125, USA
[2]Loughborough University, Wolfson School of Mechanical and Manufacturing Engineering
Loughborough University, Leicestershire, LE11 3TU, UK

Abstract

A continuum model of plasticity, Mesoscopic Field Dislocation Mechanics (MFDM), is used to study the interplay between grain size and grain orientation on the mechanical response of multicrystalline thin films undergoing plane strain tension. It is shown that the grain size dependence in the case of multicrystals is controlled by those grains which are relatively more susceptible to plastic deformation. This effect is captured to some extent by conventional crystal plasticity theory; however, the explicit incorporation of polar dislocations in the MFDM model significantly enhances the overall mechanical response as demonstrated in the paper.

1. Introduction

Over the past decade, with the advent of advanced integrated circuits and magnetic disks, there has been a substantial thrust to reduce the size of many of these electromechanical systems to the micron and sub-micron scale by fabricating components out of thin film materials. It is well known that these exceedingly small components experience large stresses during their lifetime which leads to excessive deformation and fracture. Thus, a thorough understanding of the mechanical properties of thin films and their deformation mechanisms is essential for successful design and development of small scaled components and systems. At this scale of component resolution, the geometrical dimensions are comparable in size to the material microstructural features which heavily influence the material behavior. Therefore, experiments capable of accurately characterizing the influence of the underlying microstructure on the mechanical properties are critical in our understanding of the underlying principles that drive the mechanics of small scaled components.

Several pioneering studies have experimentally identified the existence of size effects on plasticity of micron-sized polycrystalline metals under non-uniform straining, i.e. in the presence of plastic strain gradients induced by the test conditions, such as, nanoindentation

http://dx.doi.org/10.1016/j.commatsci.2011.03.001

[1], beam deflection [2] and torsion [3]. In the recent past, size effects in free-standing polycrystalline FCC thin films under nominally homogeneous axial deformation have been investigated by Espinosa and co-workers [4] by membrane deflection experiment. The yield stress of the films is observed to increase with decreasing film thickness and width. These effects were observed when there were only about two grains along the thickness of the gold samples used. However, the varying average grain size with film thickness complicates the interpretation of the observed size effect. More recently, experimental results on thin films of Copper show a strong Bauschinger effect in unloading which is also size dependent, with thinner films having a high reverse plastic strain as compared to thicker films [5].

From a modeling perspective, classical plasticity theories which have no explicit characterization of the underlying dislocations in the material cannot predict size dependence in this regime. The generally accepted size limit for accurate description of plasticity by the classical theory is systems with dimensions larger than $100\,\mu m$. At the other end of the spectrum, molecular mechanics can accurately describe material behavior but are severely limited by the computational limit of simulating individual atoms. The maximum size regimes which are computationally viable are systems with dimensions smaller than $0.5\,\mu m$ [6,7]. A continuum framework of dislocation mechanics based plasticity theory, namely, Mesoscopic Field Dislocation Mechanics (MFDM), has been proposed by Acharya and Roy [8]. In this theory, mesoscopic plasticity is modeled as an extension of conventional plasticity, which accounts for the effects of dislocation stresses as well as their spatio-temporal evolution in a physically meaningful averaged sense. Numerical results obtained from a finite element implementation of MFDM are in good qualitative agreement with experimental observations and some of the key physically relevant problems has been successfully solved and documented [9,10,11]. Motivated by the experimental observations [4,5], the effect of surface passivation, grain orientation, grain boundary constraints, and film thickness on the mechanical response of multicrystalline thin films is studied using MFDM in [12]. In this study, individual grains constituting the thin film are assumed to be of equal sizes. However, in reality, the grain size distribution in any thin film is seldom homogeneous. In this paper, we consider grains of different sizes in a multicrystalline film undergoing plane strain tension and analyze the effect of the interplay between grain size distribution and grain orientation on the loading and unloading characteristics of the thin films.

http://dx.doi.org/10.1016/j.commatsci.2011.03.001

The paper is organized as follows: a brief self contained description of the governing equations of MFDM is presented in Section 2. Section 3 comprises the problem setup followed by results and associated discussions. The paper ends with some concluding remarks in Section 4.

2. Theory

Mesoscopic field dislocation mechanics is a framework appropriate for meso length scales (less than100 μm) where the system of PDEs is obtained by averaging the equations of fine scale FDM [13]. These equations contain undetermined averages that must be modeled constitutively much in the spirit of Large Eddy Simulations (LES) of turbulence. For the convenience of the reader, the essential equations of MFDM are summarized below.

The equations prescribing the elastic incompatibility are

$$\begin{aligned} curl\,\boldsymbol{\chi} &= \boldsymbol{\alpha} \\ div\,\boldsymbol{\chi} &= \boldsymbol{0} \\ \boldsymbol{\chi}\boldsymbol{n} &= \boldsymbol{0} \qquad \partial \end{aligned} \tag{1}$$

Here, $\boldsymbol{\chi}$ is the incompatible part of the elastic distortion tensor $\boldsymbol{U}^e$, $\boldsymbol{n}$ is the unit normal on the boundary of the body ∂ and $\boldsymbol{\alpha}$ is the dislocation density tensor. The compatible part of $\boldsymbol{U}^e$ is given by $grad\,(\boldsymbol{u} - z$, where $\boldsymbol{u}$ is the total displacement field and z obeys the relation,

$$div\ grad\ \dot{:} \qquad \times \boldsymbol{V} + \boldsymbol{L} \tag{2}$$

$\boldsymbol{V}$, the averaged dislocation velocity vector, and $\boldsymbol{L}^p$ need to be specified constitutively. Roughly speaking $\boldsymbol{L}^p$ has the physical meaning of representing that part of the total plastic strain rate not represented by the slipping produced by the averaged dislocation density. The value of $\dot{:}$ is prescribed at an arbitrarily chosen point of the body and in our case assumed to vanish without loss of generality. The (symmetric) stress tensor $\boldsymbol{T}$ satisfies

$$\begin{aligned} \boldsymbol{T} &= \boldsymbol{C} \qquad \boldsymbol{u} - z + \boldsymbol{\chi} \\ div\,\boldsymbol{T} &= \boldsymbol{0} \end{aligned} \tag{3}$$

where, $\boldsymbol{C}$ is the possibly anisotropic fourth order tensor of linear elastic moduli. Standard traction/displacement boundary conditions are to be used with the above equation. Finally the temporal evolution of the dislocation density tensor field is prescribed as

$$\dot{\boldsymbol{\alpha}} \qquad \boldsymbol{S} + \boldsymbol{s} \tag{4}$$

http://dx.doi.org/10.1016/j.commatsci.2011.03.001

where $\boldsymbol{s}$ is the dislocation nucleation rate tensor to be specified constitutively and $\boldsymbol{S}$, the macroscopic slipping distortion, is defined as

$$\boldsymbol{S} := \boldsymbol{\alpha} \times \boldsymbol{V} + \boldsymbol{L} \tag{5}$$

The least restrictive boundary condition on (4) would be to impose $\boldsymbol{\alpha}\ \boldsymbol{V} \cdot \boldsymbol{n}$ on inflow points of the boundary (where $\boldsymbol{V} \cdot \boldsymbol{n} <$), with a specification of $\boldsymbol{L}^p \times \boldsymbol{n}$ on the entire boundary.

The constitutive choices of the elastic moduli $\boldsymbol{C}$ and the slipping distortion (5) introduce quantities that we model phenomenologically to complete the model. Simple choices motivated by conventional plasticity and the thermodynamics of MFDM are,

$$\begin{aligned} \boldsymbol{L}^p &= \left(\sum \cdot \right. \\ \boldsymbol{V} &= \frac{\boldsymbol{d}}{|\boldsymbol{d}|} \quad \geq \end{aligned} \tag{6}$$

where, $sym\ \bullet$ implies the symmetric part of $\bullet$, $\boldsymbol{m}_0^{\kappa}$ and $\boldsymbol{n}_0^{\kappa}$ are the unstretched unit slip direction and normal, respectively, $\boldsymbol{d}$ is the direction of the polar dislocation velocity, $\dot{\gamma}$ represents the magnitudes of SD slipping rate on the slip system κ and v is the averaged velocity of polar dislocations. The motivation behind using the symmetric part in (6) is explained in detail in Puri et al. [12]. A power law is used for $\dot{\gamma}$,

$$\dot{\gamma}^{\kappa} = \dot{\gamma}_0^{\kappa} sgn(\tau^{\kappa} - \Omega^{\kappa}) \left(\frac{|\tau^{\kappa} - \Omega^{\kappa}|}{g} \right)^{\frac{1}{m}} \tag{7}$$

where, τ^{κ} is the resolved shear stress on slip system κ, Ω^{κ} (scalar for each κ) is the back stress corresponding to the individual slip system κ, m is the rate-sensitivity of the material, g is the strength of the material, and $\dot{\gamma}_0$ is a reference strain rate on the slip system κ. The expression of back stress evolution is,

$$\dot{\Omega}^{\kappa} = \left(|\boldsymbol{\alpha}\, \boldsymbol{m}_0^{\kappa}| + |\boldsymbol{\alpha}\, \boldsymbol{p}_0^{\kappa}| \right) L \mu \dot{\gamma}^{\kappa} - c \Omega^{\kappa} |\dot{\gamma}^{\kappa}|; \boldsymbol{p}_0^{\kappa} = \boldsymbol{m}_0^{\kappa} \times \boldsymbol{n}_0^{\kappa} \tag{8}$$

where, L is the hardening coefficient and c is the recovery coefficient. The resolved shear stress τ^{κ} is,

$$\tau^{\kappa} = \boldsymbol{m}_0^{\kappa} \cdot \boldsymbol{T} \boldsymbol{n}_0^{\kappa} \tag{9}$$

The direction of polar dislocation velocity, $\boldsymbol{d}$ is,

http://dx.doi.org/10.1016/j.commatsci.2011.03.001

$$\boldsymbol{d} := \boldsymbol{b} - \left(\boldsymbol{b} \cdot \frac{\boldsymbol{a}}{|\boldsymbol{a}|}\right)\frac{\boldsymbol{a}}{|\boldsymbol{a}|},$$
$$\boldsymbol{b} := \boldsymbol{X}\left(\boldsymbol{T}'\boldsymbol{\alpha}\right) \;;\; b_i = e_{ijk}T'_{jr}\alpha_{rk} \quad ; \quad \boldsymbol{a} := \boldsymbol{X}\left(tr\left(\boldsymbol{T}\right)\boldsymbol{\alpha}\right) \;;\; a_i = \left(\frac{1}{3}T_{mm}\right)e_{ijk}\alpha_{jk}. \tag{10}$$

The expression for v is assumed to be

$$v\left(state\right) = \frac{\eta^2 b}{n_{slip}}\left(\frac{\mu}{g}\right)^2 \sum_{\kappa} \dot{\gamma}^{\kappa} \tag{11}$$

where μ is the shear modulus, b the Burgers vector magnitude, n_{slip} is the total number of slip systems and $\eta =$ a material parameter. The strength of the material is assumed to evolve according to,

$$\dot{g} = \left[\frac{\eta^2 \mu^2 b}{2\left(g - g_0\right)} k_0 \left|\boldsymbol{\alpha}\boldsymbol{n}_0^{\kappa}\right| + \theta_0\left(\frac{g_s - g}{g_s - g_0}\right)\right]\left\{\left|\boldsymbol{\alpha} \times \boldsymbol{V}\right| + \sum_{\kappa} \dot{\gamma}^{\kappa}\right\} \tag{12}$$

where g_s is the saturation stress, g_0 is the yield stress, and θ_0 is the Stage II hardening rate. k_0 is an extra parameter in the MFDM model that needs to be fitted experimentally. The boundary conditions, initial conditions and details of the numerical implementation of the equations using the Finite Element Method are described in [9,12,13].

3. Results and Discussion

An unpassivated multicrystalline thin film with fully penetrable grain boundaries and different grain sizes (lateral dimension), is considered. Two specific grain geometries are modeled and are shown in Figure 1. Film 1 consists of 4 grains of equal dimensions. In film 2, the number of grains is the same as in film 1 but with different lateral dimensions. For both films, the grain thickness equals the overall film thickness ($h =$). The chosen dimensions of the thin film are motivated from the physical experiments carried out by Xiang and Vlassak [5]. All samples are initially unstressed and dislocation free. In order to critically assess the effect of individual grain orientation on the overall deformation characteristics of the considered films, three different sets of grain orientations are considered:

(a) Orientation Set 1: the misorientation between adjacent grains is 3-5 degrees about the x_3-axis,

http://dx.doi.org/10.1016/j.commatsci.2011.03.001

(b) Orientation Set 2: misorientation between adjacent grains is 20-30 degrees about the x_3-axis, and

(c) Orientation Set 3: misorientation between adjacent grains is assumed to be the same as Orientation Set 2 however the sequence of grain misorientation is varied.

The Euler angles corresponding to different orientation sets are tabulated in Table 1. Material parameters representative of Copper are used for all the numerical experiments conducted except for k_0, L and c, for which we make the choice of $k_0 =$, $L = 100\ \mu$m, $c =$ motivated by Puri et al. [12]. The other material parameters used are $b = 2.5 \times 10^{-4}\ \mu$m, $m =$ $g_s =$ a, $g_0 =$ ı, and $\theta_0 =$ a. The reference strain rate is $\dot{\gamma}$ Isotropic elastic constants of the material are $E =$ a, $\nu =$ where E is the Young's modulus and ν is the Poisson's ratio.

A regular mesh of 16× × elements in x_1, x_2, x_3 directions is used to discretize the chosen film geometry. Figure 1 is a schematic sketch of the film samples modeled. Boundary conditions are applied in order to simulate a plain strain tension deformation mode in the film body as follows:

$u_1 = 0$ at $x_1 = 0$

$u_2 = 0$ at $x_2 = 0$

$u_3 = 0$ at $x_3 = w$

where, w is the width of the specimen in the x_3 direction. The surfaces at $x_1 =$ and $x_1 =$ are traction free in the x_2, x_3 directions. The surface at $x_2 =$ is traction free in the x_1, x_3 directions and the surface at $x_2 =$ is traction free in the x_1, x_2, x_3 directions. The surface at $x_3 = w$ is traction free in the x_1, x_2 directions. Displacements corresponding to plane strain tension are prescribed through the kinematic boundary condition,

$$u_1(x_1, x_2, x_3, t) = 4d\dot{\varepsilon}\, t \tag{13}$$

on the nodes of the surface at $x_1 =$. Here, $4d$ is the edge length of the specimen in x_1 direction, $\dot{\varepsilon}$ is an applied tensile strain rate of $1\ \text{sec}^{-1}$, and t is time. All degrees of freedom on the surface at $x_3 =$ are set to be equal to the value of corresponding degrees of freedom on the surface at $x_3 = w$. All components of the polar dislocation density ($\boldsymbol{\alpha}$) on the

http://dx.doi.org/10.1016/j.commatsci.2011.03.001

left external face at $x_1 =$ are set to be equal to the components of corresponding nodes on the right face at $x_1 =$. This implies that the flow of dislocations on the right face is equal and opposite to that on the left face

$$\boldsymbol{\alpha}\big|_L = \boldsymbol{\alpha}\big|_R \tag{14}$$

In the plots and rest of the text, volume average of $\boldsymbol{T}$ in the 11 direction is denoted by $\boldsymbol{\sigma}$ with the "-" sign representing a compressive stress and "+" sign representing a tensile stress.

3.1 Orientation Set 1

In this section we study the consequence of a low misorientation angle in adjacent grains of the thin film for the two representative grain size distributions chosen. Displacement corresponding to an engineering tensile strain of 0.675% is imposed on the film sample during the loading step. Subsequently, the film is unloaded to a net imposed strain of 0%.

The overall average stress-strain response for different sets of grain geometries is shown in Figure 2. It is observed that there is no significant effect of the variation of the lateral grain size on the mechanical response of the films considered in both conventional plasticity and MFDM. However the MFDM analysis clearly demonstrates a noticeable harder response in loading. This observation comes as no surprise as conventional plasticity with no explicit characterization of dislocations is unable to account for the excess dislocation distributions which MFDM has been shown to account for accurately [9,12].

The lack of any noticeable distinction between the response of considered individual film configurations is due to the low misorientation angle between individual grains which leads to the overall thin film to closely represent a single crystal orientation irrespective of lateral grain size distribution. During the unloading step, unlike the MFDM framework classical plasticity formulation predicts no Bauschinger effect (Figure 2).

3.2 Orientation Set 2

The misorientation angle between the individual grains of the thin films studied is now increased to 20-30 degrees (Table 1). The stress-strain plot corresponding to this orientation set is shown in Figure 3. It is observed that films 1 and 2 demonstrate a distinct difference with respect to the overall stress-strain response in the classical plasticity framework. This is to be expected as classical plasticity accounts for the specific slip plane orientations which

http://dx.doi.org/10.1016/j.commatsci.2011.03.001

allow plastic flow to occur. The nominal response of the film is purely an effect of the deformation response of individual grain orientation in the film cases studied. In MFDM this difference is noticeably amplified.

MFDM demonstrates a strong Bauschinger effect during unloading in both the film configurations (Figure 3). This is due to the accumulation of polar dislocations along grains boundaries as the misorientation between adjacent grains is high in this orientation set. This feature is discussed in detail in Puri et al. [12].

3.3 Orientation Set 3

So far, we have studied the effect of an inhomogeneity in the grain size distribution on the mechanical response of a multicrystal. It may be argued from the numerical experiments discussed above that between the two film configurations studied the stress-strain response is critical only in the cases with high misorientation between adjacent grains. Additionally, film 2 demonstrated a softer response in loading and a relatively small Bauschinger effect when compared to film 1 in the context of Orientation Set 2. Performing a dimensional analysis of σ in the context of MFDM, we find that,

$$\sigma = \left(\right) \tag{15}$$

where, α_0 is the magnitude of the initial polar dislocation density field, s is a representative measure of distribution of grain size, H is the external dimension of the body and Φ is a dimensionless function of the arguments shown. In the above expression, s/H introduces a dependence of the average response on the grain size distribution. However, the nature of dependence is not clear from the dimensional analysis. The motivation behind orientation set 3 is to understand this interplay between grain orientation and grain size in the case of a multicrystal with high misorientation between adjacent grains.

In terms of grain geometry, two grains in film 2 is larger and two smaller in comparison to film 1. It is evident from Figure 4(a) and (c), that plastic deformation is dominant in grain 2 in films 1 and 2, respectively in orientation set 2. The softening response is due to the fact that the grain with dominant plasticity is larger in volume in film 2. To prove this hypothesis, we study a test case in which the grain orientation of grain 1 and 2, and grain 3 and 4 is swapped as mentioned in Table 1. Figure 5 demonstrates the stress-strain plot of the swapped

http://dx.doi.org/10.1016/j.commatsci.2011.03.001

grain case using MFDM model. It is observed that in this case, film 2 shows a stronger response in comparison to film 1. Additionally, a higher Bauschinger effect is also observed in film 2. This is entirely due to the fact that the grain with dominant plasticity has become smaller in this case.

4 Concluding Remarks

A numerical implementation of MFDM has been used to demonstrate the influence of grain orientation and grain size on the overall macroscopic response of thin films. In an unconstrained film with no passivation layer and no constraints on plastic flow through grain boundaries, there is a strong effect of the interaction between slip plane orientation and grain size on the plastic deformation. The exact nature of plastic flow across grain boundaries plays a critical role in the overall mechanical response of thin films, coupled with the orientation of individual grains in the body. Our continuum framework allows for the accurate modeling of grain boundaries with a physical mechanism for modeling dislocation induced plasticity in crystalline materials. The critical interplay between the grain boundary constraints and the grain orientation has been mentioned briefly in [12] and will be reported in detail for specimens with dimensions of tens of microns and large number of grains in the near future.

References

[1] Q. Ma, D.R. Clarke. Journal Of Materials Research, 10 (4) (1995) 853-863.
[2] J.S. Stölken, A.G. Evans. Acta Materialia, 46 (14), (1998) 5109-5115.
[3] N.A. Fleck, G.M. Muller, M.F. Ashby, J.W. Hutchinson. Acta Metallurgica Et Materialia, 42, (1994) 475-487.
[4] H.D. Espinosa, B.C. Prorok, , B. Peng, . Journal of the Mechanics and Physics of Solids. 52, (2004) 667 – 689.
[5] Y. Xiang, J.J. Vlassak. Acta Materialia. 54 (2006)5449-5460.
[6] R.K. Rajgarhia, D.E. Spearot, A. Saxena. Journal of Materials Research, 25,3, (2010) 421
[7] D.E. Spearot, D.L. McDowell. Journal of Engineering Materials and Technology, 131 (2009)
[8] A. Acharya, A. Roy. Journal of the Mechanics and Physics of Solids. 54, (2006) 1687-1710.
[9] A. Roy, A. Acharya. Journal of the Mechanics and Physics of Solids. 54 (2006) 1711-1743.
[10] S. Puri. Ph.D. Thesis, Carnegie Mellon University (2009)
[11] S. Puri, A. Roy, A. Acharya, D. Dimiduk Journal of Mechanics of Materials and Structures. 4, (2010) 1603-1618.

http://dx.doi.org/10.1016/j.commatsci.2011.03.001

[12] S. Puri, A. Das, A. Acharya. *Submitted to* Journal of the Mechanics and Physics of Solids, (2010)
[13] A. Roy, A. Acharya. Journal of the Mechanics and Physics of Solids. 53 (2005) 143-170.

http://dx.doi.org/10.1016/j.commatsci.2011.03.001

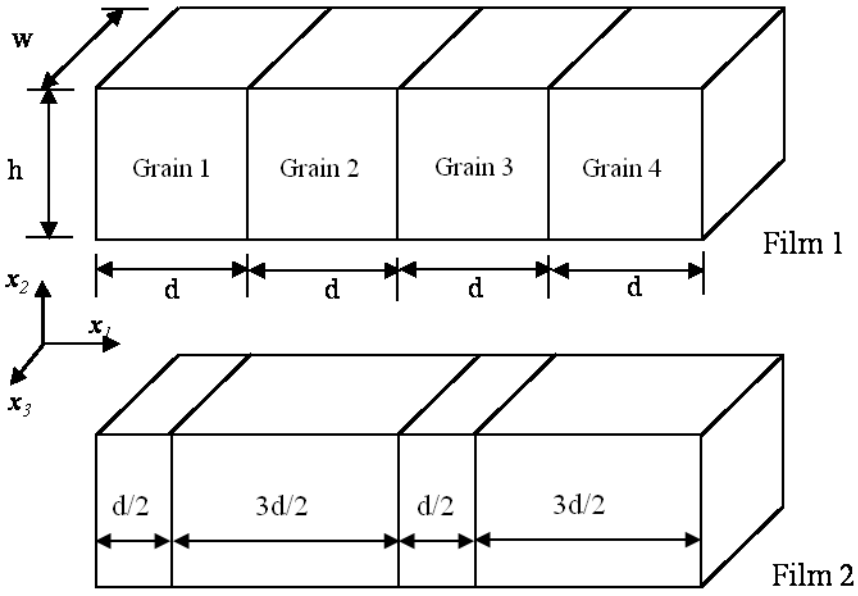

Figure 1. Grain geometry of films 1 and 2.

Table 1. Euler angles of four grains in diffferent orientation sets (in degrees)

Orientation Set	**Grain 1**	**Grain 2**	**Grain 3**	**Grain 4**
1	(5,0,0)	(2,0,0)	(4,0,0)	(7,0,0)
2	(25,0,0)	(4,0,0)	(40,0,0)	(15,0,0)
3	(4,0,0)	(25,0,0)	(15,0,0)	(40,0,0)

http://dx.doi.org/10.1016/j.commatsci.2011.03.001

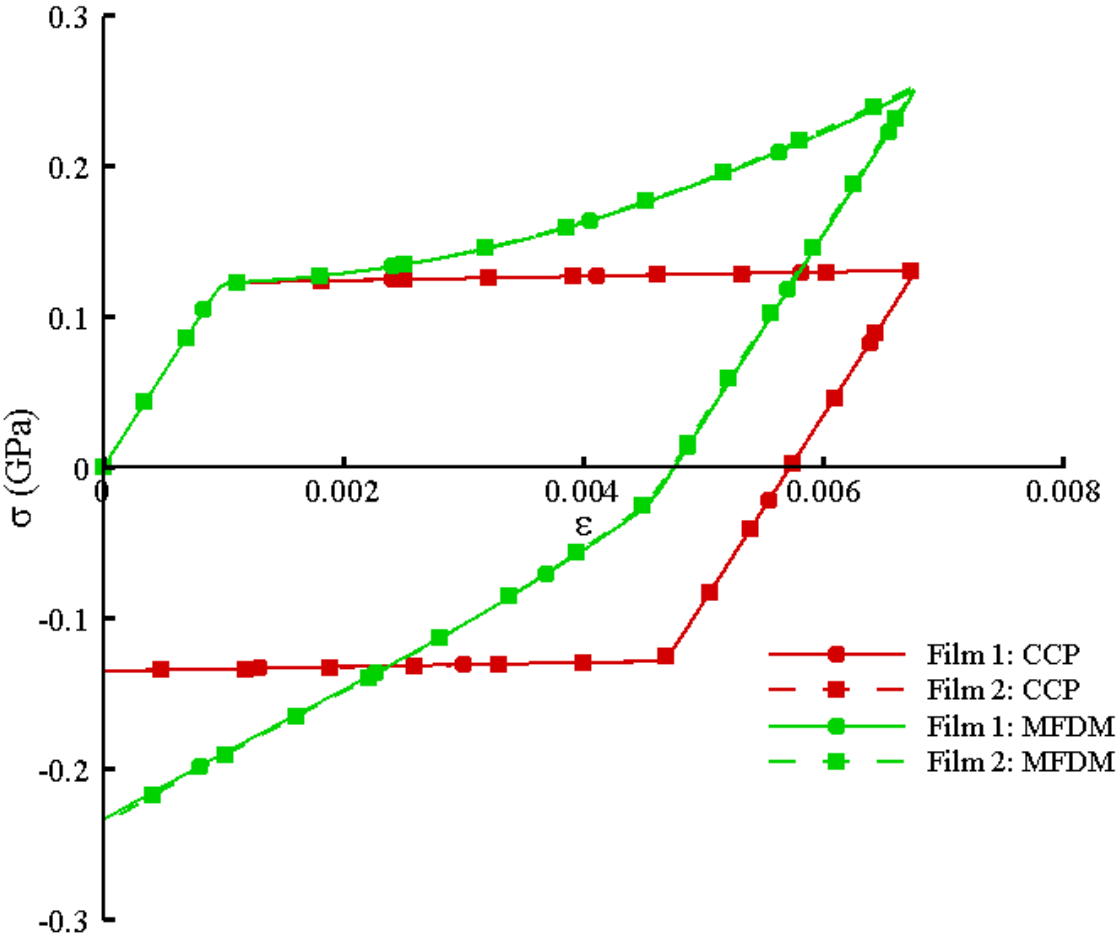

Figure 2. Stress-strain behavior of thin films for the orientation set 1 (CCP = Conventional Crystal Plasticity)

http://dx.doi.org/10.1016/j.commatsci.2011.03.001

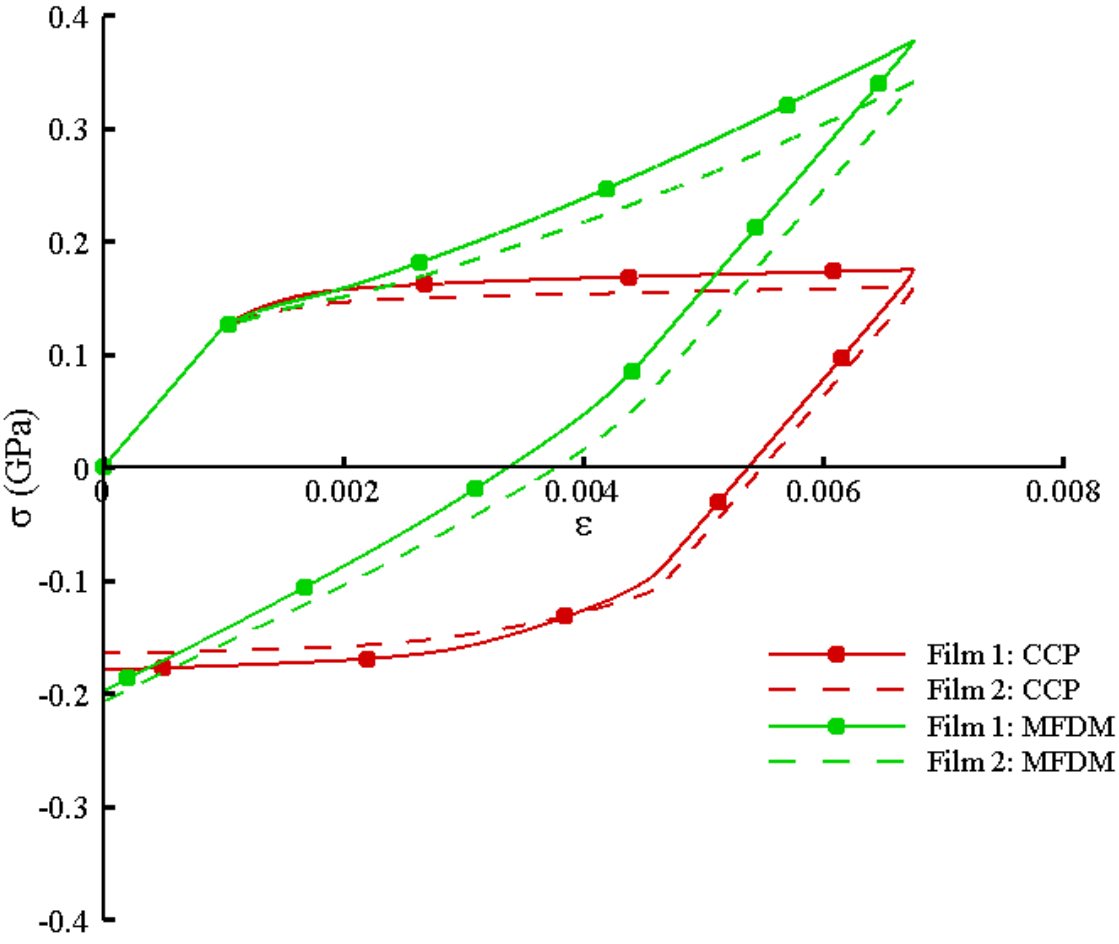

Figure 3. Stress-strain behavior of thin films for the orientation set 2 (CCP = Conventional Crystal Plasticity)

http://dx.doi.org/10.1016/j.commatsci.2011.03.001

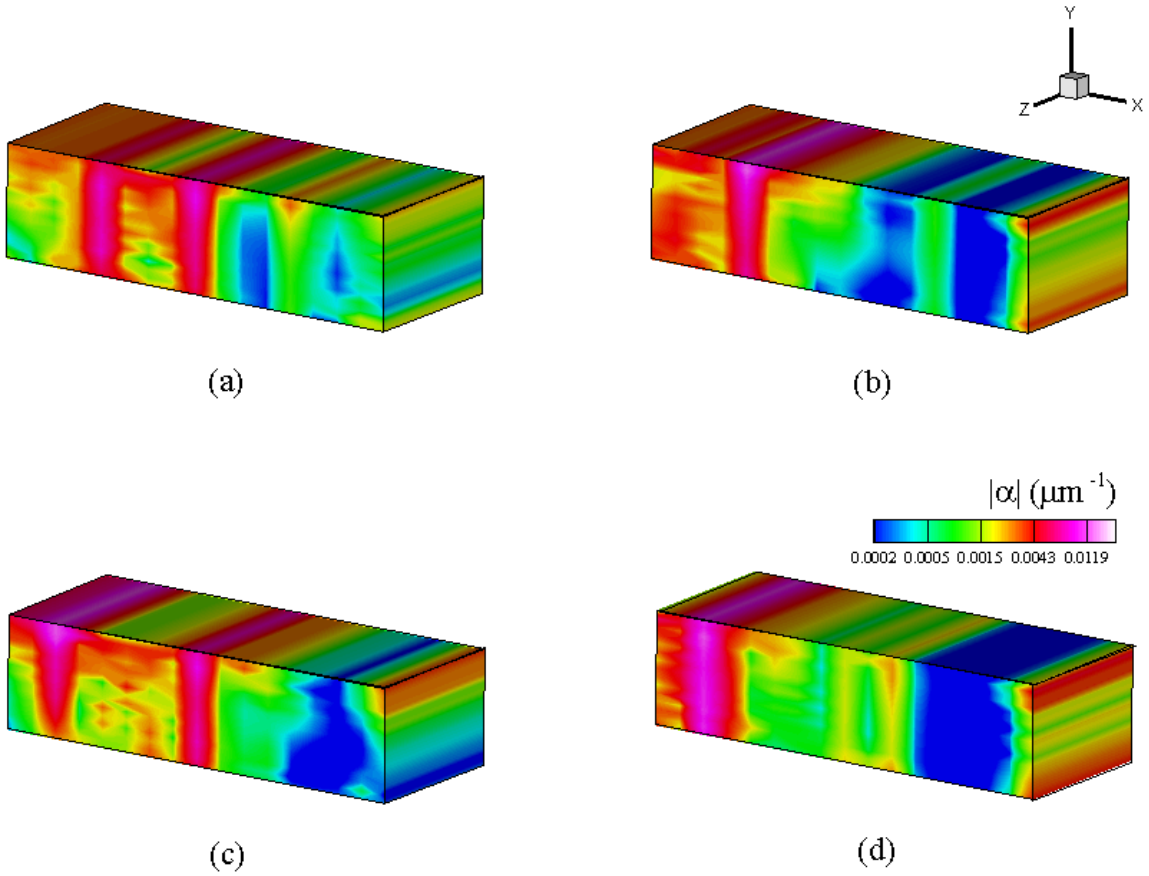

Figure 4. Field plot of $|\alpha|$ at 0.15% applied strain; (a) Film 1 with orientation set 2, (b) Film 1 with orientation set 3, (c) Film 2 with orientation set 2, and (d) Film 2 with orientation set 3.

http://dx.doi.org/10.1016/j.commatsci.2011.03.001

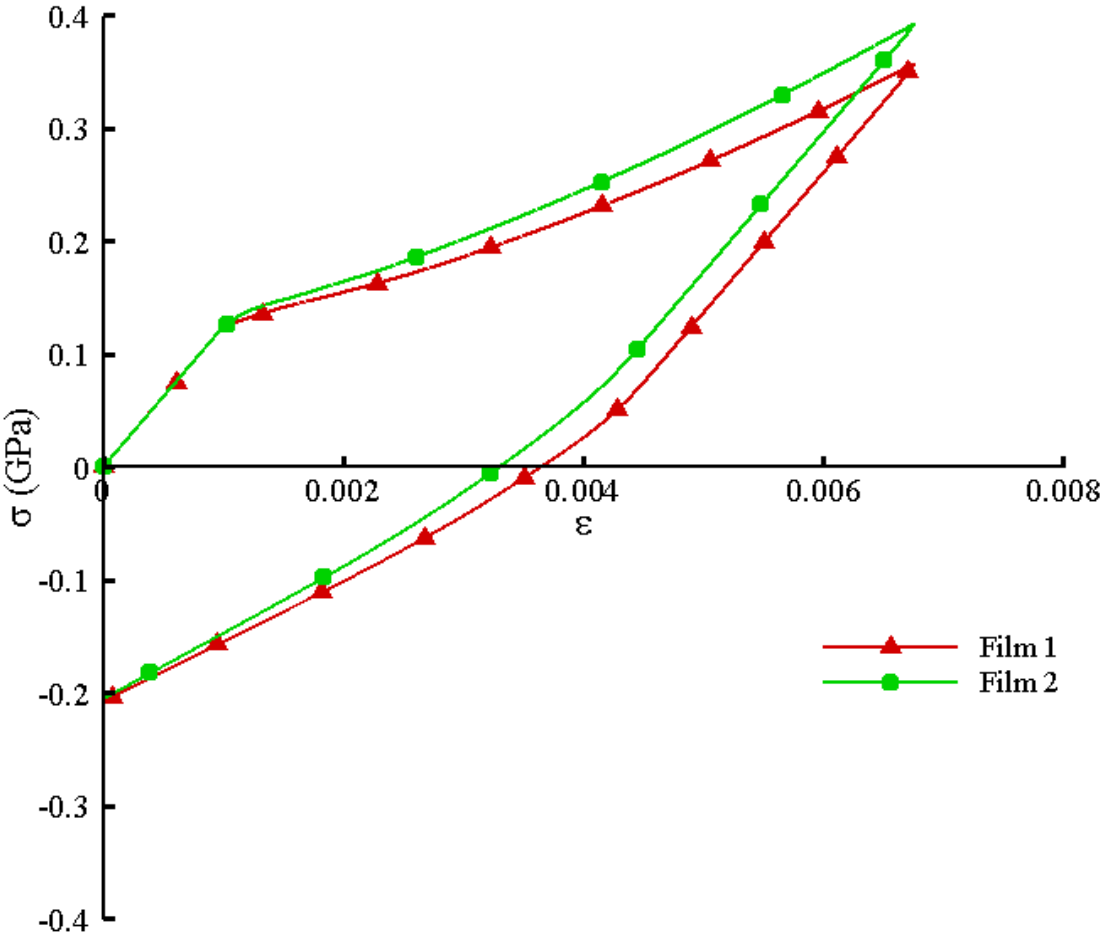

Figure 5. Stress-strain behavior of thin films for the orientation set 3.